Eur. Phys. J. B **43**, 53–64 (2005)
DOI: 10.1140/epjb/e2005-00027-5

THE EUROPEAN PHYSICAL JOURNAL B

Lattice vibrational analysis of polyacene

H. Zhao[1], Z. An[1,2], and C.Q. Wu[1,a]

[1] Department of Physics, Fudan University, 200433 Shanghai, P.R. China
[2] College of Physics, Hebei Normal University, 050016 Shijiazhuang, P.R. China

Received 27 October 2004
Published online 11 February 2005 –

Abstract. Within an extended Su-Schrieffer-Heeger model, we made a lattice vibrational analysis of polyacene. In a singly-charged polyacene, the ground state contains an interchain-coupled polaron of quasi-D_{2h} symmetry, around which we found thirteen localized modes in total. Among these localized modes, five (three B_{2u} and two B_{3u}) are infrared active, six (four A_g and two B_{1g}) modes are Raman active, and the other two localized modes are asymmetric, which are both infrared active and Raman active. For the case a charged polaron is coupled with a neutral soliton in a finite polyacene chain, the vibrational modes are also calculated to display the coupling effect between self-trapping excitations on phonons. It is found that the localized phonons are determined mainly by the charged polaron, but the number and frequencies of the localized modes are influenced by the existence of the neutral soliton.

PACS. 63.22.+m Phonons or vibrational states in low-dimensional structures and nanoscale materials – 63.20.Pw Localized modes

1 Introduction

There have been considerable amounts of research works devoted to the properties of nonlinear elementary excitations in conjugated polymers, such as soliton, polaron and polaron-exciton [1,2]. The motivation behind these works stems from the fact that these excitations play an important role in optoelectric devices based on conjugated polymers, including field-effect transistors, light-emitting diodes, photocells and lasers [3–9]. The localized phonon modes can be considered as the fingerprint [10,11] of these nonlinear excitations, therefore, it is very interesting to investigate the vibrational modes in order to understand dynamic properties of various self-trapping elementary excitations in conjugated polymers.

Polyacene, as a novel conducting polymer, has long been the focus of theoretical studies [9,10,12–24], though a long polyacene chain has not been synthesized yet. Polyacene, linearly fused aromatic rings, can be considered as two polyacetylene chains strongly coupled by cross alternate interactions. Much theoretical works have been devoted to the ground state of an infinite polyacene chain [12–19], that is the polyacene composed of an infinite-number aromatic rings with a periodic boundary condition (PBC), where the ground state of a neutral polyacene is perfectly dimerized and an interchain-coupled polaron exists in a singly-charged polyacene. In an earlier paper [23], we have investigated the self-trapping excitations and absorption spectrum of a polyacene chain composed of a finite-number aromatic rings with open boundary condition (OBC). With the OBC, while an interchain neutral soliton was found in a pristine polyacene chain, there exist an interchain polaron being coupled with the neutral soliton in a singly charged polyacene chain [23]. In a previous paper [10], we have primarily investigated the localized phonon modes around the interchain neutral soliton and gave out quite different results from that in polyacetylene. In this paper, we will report a systematic investigation on the phonon modes of a singly charged polyacene chain, which is composed of aromatic rings with either the OBC or the PBC. While the localized phonon modes around the interchain-coupled polaron are obtained by a numerical method, the extended phonon spectra are given out analytically in a pristine polyacene chain with the PBC. Finally, the coupling effect of the neutral soliton and the charged polaron on localized phonon modes is figured out.

This paper is organized as follows. The theoretical model and numerical method employed in this work are described in Section 2. The numerical results are given in Sections 3 and 4. Then a summary is given in Section 5 and an analytic evolution on the extended phonon spectra is given in the Appendix.

2 Model and method

Since a polyacene chain can be considered as two polyacetylene chains with alternate interchain coupling, we use the following extended Su-Schrieffer-Heeger model [10,20–23]:

$$H = H_e + H_{int} + H_p, \tag{1}$$

[a] e-mail: cqw@fudan.edu.cn

where

$$H_e = -\sum_{j,n,\sigma}[t_0+\alpha(u_{j,n}-u_{j,n+1})](c^{\dagger}_{j,n,\sigma}c_{j,n+1,\sigma}+\text{h.c.}) \quad (2)$$

describes the intra-chain interactions,

$$H_{int} = -\sum_{n,\sigma}[t_1-(-1)^n t_2](c^{\dagger}_{1,n,\sigma}c_{2,n,\sigma}+\text{h.c.}) \quad (3)$$

describes the interchain interactions, and

$$H_p = \frac{1}{2}K\sum_{j,n}(u_{j,n}-u_{j,n+1})^2+\frac{1}{2}M\sum_{j,n}\dot{u}^2_{j,n} \quad (4)$$

gives the lattice elastic and kinetic energies. In equations (2−4), j (= 1, 2) denotes the chain index, the quantity t_0 is the transfer integral for π-electrons in a regular lattice, α the electron-lattice coupling constant, and $u_{j,n}$ the lattice displacement of the nth site on chain j from its equidistant position. The operator $c^{\dagger}_{j,n,\sigma}(c_{j,n,\sigma})$ creates (annihilates) a π-electron with spin σ at the n-th site on chain j, and K the elastic constant due to the σ-bonds. t_1 and t_2 describe the alternate interchain interactions, and $t_1 = t_2$ corresponds to the case of polyacene. Ab initio calculations on short polyacene chains have shown that the bonds between the two chains are slightly longer than the single bond in the chain, so we would like to use $2t_1 = 0.864t_0$ in our calculations. The other quantities are taken as follows [10,20–23]: $t_0 = 2.5$ eV, $\alpha = 4.1$ eVÅ^{-1}, $K = 15.5$ eVÅ^{-2}; then the dimensionless electron-lattice coupling constant $\lambda(\equiv 2\alpha^2/\pi t_0 K) = 0.276$, which is larger than that for polyacetylene [2].

For the Peierls ground state of a polyacene chain with PBC, we have $u_{j,n} = (-1)^n u_0^{(j)}$, like the case of polyacetylene, where the electronic part of the Hamiltonian in (1) can be diagonalized by the Bogoliubov transformation (for details, see Appendix). The energy spectrum is the same for both the alternate *cis* ($u_0^{(1)} \equiv u_0^{(2)}$) and *trans* ($u_0^{(1)} \equiv -u_0^{(2)}$) configurations [23]. It has been known [10,23] that the bond configuration will be always in the *cis*-phase, i.e., $u_{j,n} \equiv u_n$ ($j = 1, 2$) for a polyacene chain with the OBC since the edge bonds should be shorter. For this reason, we will only consider the *cis*-phase with either the PBC or the OBC, where the electronic wavefunctions must be either symmetric $\phi(1,n) = \phi(2,n) = \phi^{(s)}(n)$ or anti-symmetric $\phi(1,n) = -\phi(2,n) = \phi^{(a)}(n)$ for the two chains of polyacene. We define the bond order parameter δ_n by $\delta_n = (-1)^n(u_{n+1}-u_n)$, then the Hamiltonian (1) can be solved self-consistently using the following coupled equations to obtain the static bond configuration and the electronic wave functions:

$$\varepsilon^{(\kappa)}_{\mu}\phi^{(\kappa)}_{\mu}(n) = -[t_0-(-1)^n\alpha\delta_n]\phi^{(\kappa)}_{\mu}(n+1)$$
$$-[t_0+(-1)^n\alpha\delta_{n-1}]\phi^{(\kappa)}_{\mu}(n-1)-\eta_{\kappa}[t_1-(-1)^n t_2]\phi^{(\kappa)}_{\mu}(n), \quad (5)$$

$$\delta_n = (-1)^{n+1}\frac{2\alpha}{K}$$
$$\times\sum_{\mu(occ.)}\left[\phi^{(\kappa)}_{\mu}(n)\phi^{(\kappa)}_{\mu}(n+1)-\frac{1}{2m}\sum_n\phi^{(\kappa)}_{\mu}(n)\phi^{(\kappa)}_{\mu}(n+1)\right], \quad (6)$$

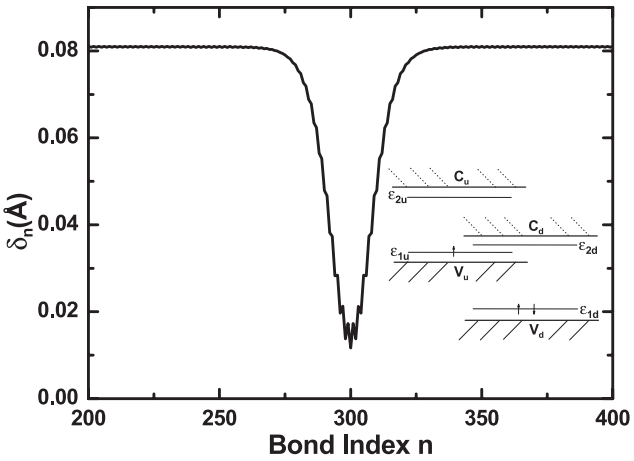

Fig. 1. Bond alternation parameters δ_n of an interchain-coupled polaron in a singly-charged polyacene chain with the PBC. The inset shows a schematic representation of the electronic energy spectrum.

where $\kappa = s, a$. $\eta_s = 1$ for symmetric states $\phi^{(s)}_{\mu}$ and $\eta_s = -1$ for anti-symmetric states $\phi^{(a)}_{\mu}$. The summation over occupied states is for both symmetric and anti-symmetric states; the last term in equation (6) comes from the Lagrange multiplier which is introduced to keep the total chain length unchanged – that is, $\sum_n(-1)^n\delta_n = 0$, and the wavefunctions $\phi^{(\kappa)}_{\mu}(n)$ has the following properties:

$$\sum_n \phi^{(\kappa)}_{\mu}(n)\phi^{(\kappa)}_{\nu}(n) = \delta_{\mu\nu}/2, \quad \sum_{\mu}\phi^{(\kappa)}_{\mu}(m)\phi^{(\kappa)}_{\mu}(n) = \delta_{mn}/2. \quad (7)$$

Then the ground state can be written as

$$|G\rangle = \prod_{\mu,\sigma(occ.)} a^{(\kappa)\dagger}_{\mu,\sigma}|0\rangle, \quad (8)$$

where

$$a^{(\kappa)\dagger}_{\mu,\sigma} = \sum_n \phi^{(\kappa)}_{\mu}(n)(c^{\dagger}_{1,n,\sigma}+\eta_{\kappa}c^{\dagger}_{2,n,\sigma}), \quad (9)$$

$$c^{\dagger}_{j,n,\sigma} = \sum_{\mu}\left[\phi^{(s)}_{\mu}(n)a^{(s)\dagger}_{\mu,\sigma}+(3-2j)\phi^{(a)}_{\mu}(n)a^{(a)\dagger}_{\mu,\sigma}\right]. \quad (10)$$

By solving numerically above self-consistent equations (5) and (6), we obtain Figure 1, which shows the bond configuration $\{\delta_n\}$ of an interchain-coupled polaron [20], with a schematic representation of the energy spectrum given as the inset, for a singly-charged polyacene chain with the PBC. As a comparison, we show in Figure 2 the bond configuration of a polaron being coupled with an interchain-coupled soliton for a singly-charged polyacene chain with the OBC [23]. Due to the existence of an interchain-coupled soliton, two more localized electronic levels appear in the electronic spectrum, while the other four localized levels are caused by the interchain-coupled polaron as those in the polyacene chain with PBC. Among the four states, two (ε_{1u} and ε_{2d}) appear in the gap while the other (ε_{1d} and ε_{2u}) appear in the valence and conduction bands, respectively. On the other hand, the bond configuration of a polyacene chain with the OBC has a symmetry of D_{2h} [10], it has only a quasi-D_{2h} symmetry

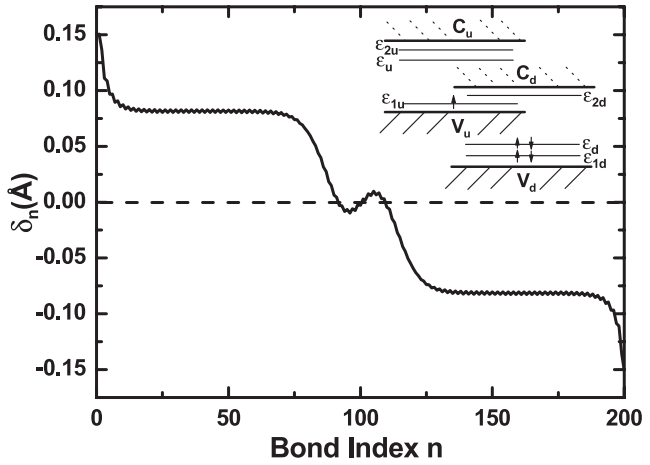

Fig. 2. Bond alternation parameters δ_n of a polaron being coupled with an interchain-coupled soliton in a singly-charged polyacene chain with the OBC. The inset shows a schematic representation of the electronic energy spectrum.

in a polyacene chain with PBC since the center of the polaron is not yet on the sites, but on the bonds.

Now we consider a small departure $\{d_{j,n}\}$ of atoms from the self-consistent bond configuration $\{\delta_n\}$, – that is, $u_{j,n} = u_n + (-1)^n d_{j,n}$; then we can do the perturbation order by order, as in reference [10]. The vanishing of the first-order term in the total energy gives the self-consistent equations (5) and (6). The second-order term of the total energy gives the vibrational Hamiltonian, which can be written as

$$H_{vib} = 2K \sum_{\kappa=s,a} \sum_{n,n'} A^{(\kappa)}_{n,n'} d^{(\kappa)}_n d^{(\kappa)}_{n'} + \frac{1}{2} M \sum_{\kappa=s,a} \sum_{n} (\dot{d}^{(\kappa)}_n)^2, \tag{11}$$

where the elements of the vibrational matrices are as follows:

$$A^{(\kappa)}_{n,n'} = \frac{1}{4}(\zeta_n \delta_{n,n'} + \delta_{n,n'\pm 1}) + \frac{1}{2}\lambda \pi t_0 (-1)^{n+n'} \times \left(\Xi^{(\kappa)}_{n,n'} - \Xi^{(\kappa)}_{n,n'-1} - \Xi^{(\kappa)}_{n-1,n'} + \Xi^{(\kappa)}_{n-1,n'-1} \right), \tag{12}$$

where $\zeta_n = 1$ for n being sites at chain ends and $\zeta_n = 2$ for n being all other sites, and

$$\Xi^{(s)}_{n,n'} = \sum_{\mu(occ.),\nu(unocc.)} \sum_{\kappa=s,a} \frac{\chi^{\kappa\kappa}_{\mu,\nu}(n)\chi^{\kappa\kappa}_{\mu,\nu}(n')}{\varepsilon^{(\kappa)}_\mu - \varepsilon^{(\kappa)}_\nu},$$
$$\Xi^{(a)}_{n,n'} = \sum_{\mu(occ.),\nu(unocc.)} \sum_{\kappa=s,a} \frac{\chi^{\kappa\overline{\kappa}}_{\mu,\nu}(n)\chi^{\kappa\overline{\kappa}}_{\mu,\nu}(n')}{\varepsilon^{(\kappa)}_\mu - \varepsilon^{(\overline{\kappa})}_\nu}, \tag{13}$$

where $\kappa = s, \overline{\kappa} = a$ and $\kappa = a, \overline{\kappa} = s$, and

$$\chi^{\kappa\kappa'}_{\mu,\nu}(n) = \phi^{(\kappa')}_\nu(n)\phi^{(\kappa)}_\mu(n+1) + \phi^{(\kappa')}_\nu(n+1)\phi^{(\kappa)}_\mu(n). \tag{14}$$

So we have the phonon frequency $\omega^{(\kappa)}$ from $(\omega^{(\kappa)})^2 = \omega_Q^2 \lambda^{(\kappa)}$, where $\lambda^{(\kappa)}$ are the eigenvalues of the vibrational matrix $\{A^{(\kappa)}_{n,n'}\}$ given in equation (12) and $\omega_Q = \sqrt{4K/M}$ is the bare phonon frequency, which is about 1900 cm^{-1} for polyacene.

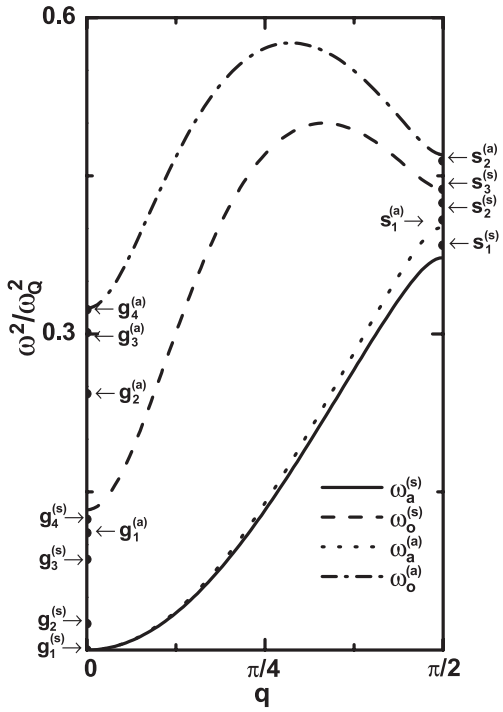

Fig. 3. The phonon spectrum of a singly-charged polyacene chain with the PBC. The energies of the localized modes around the polaron are indicated by arrows.

3 Localized phonons around an interchain-coupled polaron

For a singly-charged polyacene chain with the PBC, an interchain-coupled polaron has been obtained [20], the staggered order parameter of the polaron, $\{\delta_n\}$, has shown in Figure 1, and the schematic representation of the energy spectrum is given in the inset. Accompanying with the polaron, four extended electronic levels become localized. The diagonalization of the vibrational matrix $A^{(\kappa)}_{n,n'}$ gives both the eigenvalue $\lambda^{(\kappa)}$ and the vibrational eigenwavefunction $d^{(\kappa)}(n)$. To identify the localized modes, we define the localization factor $\gamma = \sum_n |d(n)|^4 / \sum_n |d(n)|^2$ (m is the number of aromatic rings in the polyacene chain we considered), which will decay as $1/m$ for an extended vibrational mode when the size m becomes larger and larger, while it will approach a nonzero constant for a localized vibrational mode. We have done the calculations from $m = 100 - 300$, and a very good convergence for the localization factor is reached for a polyacene composed of $m = 300$ aromatic rings, for which all results presented below are obtained.

Totally, thirteen localized modes around the interchain-coupled polaron have been found. Their energy positions in the phonon spectrum are shown in Figure 3, in which lines represents the dispersion of extended modes, which should be independent of local distortions, then we can obtain them by the calculation in the dimerized lattice in Appendix. In contrast to the polyacene chain with the OBC, such as the soliton case [10] where the structure is of a D_{2h} symmetry and the center of the soliton is located on a carbon atom,

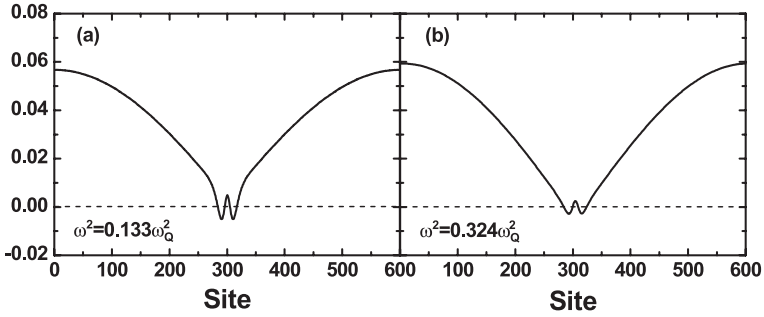

Fig. 4. The extended modes with the lowest frequency in the optical branches in the presence of a polaron, (a) $\omega_o^{(s)}(0)$ for the symmetric optical branch and (b) $\omega_o^{(a)}(0)$ for the anti-symmetric optical branch.

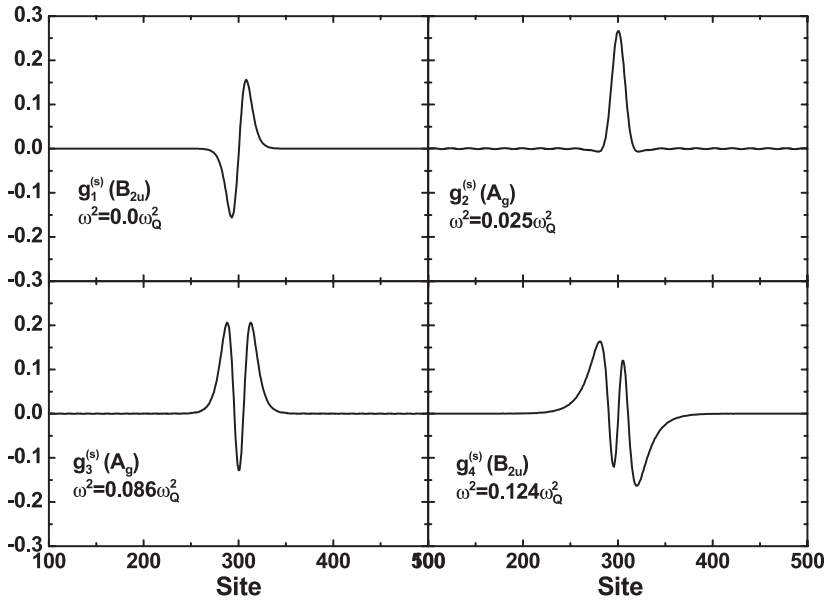

Fig. 5. Symmetric localized slowly varying phonon modes ($q = 0$) around a polaron in a singly-charged polyacene chain with the PBC.

the center of the polaron in a polyacene chain with the PBC is located on a bond. Therefore, strictly speaking, the polaron has broken the D_{2h} symmetry due to the alternate interchain coupling. Fortunately, if we discard the difference on the nearest neighbor carbons due to the alternative interchain hoppings between the two chains, the polaron possesses the D_{2h} symmetry. In this sense, we call the polaron of a quasi-D_{2h} symmetry. Similarly, there are only four one-dimensional irreducible representations A_g, B_{1g}, B_{2u}, and B_{3u} for the model that we are considering for a polyacene chain with the PBC, and the phonon modes corresponding to B_{2u} and B_{3u} are infrared active while the modes corresponding to A_g and B_{1g} are Raman active, as the soliton case [10]. As discussed below, most of vibrational modes can be identified with one of the four one-dimensional irreducible representations.

The extended modes with the lowest frequency in the optical branches in the presence of a polaron, $\omega_o^{(s)}(0)$ and $\omega_o^{(a)}(0)$, are shown in Figure 4, the energies are $\omega^2/\omega_Q^2 = 0.133$ and 0.324, respectively, which are same as that obtained by the expressions for a dimerized lattice in the Appendix. In the weak-coupling model of polyacetylene, $\omega_o^2/\omega_Q^2 = 2\lambda$, which has a value of 0.552 for polyacene. Our results are much smaller than that value; this is clearly a result of the reduction of the dimerization due to the interchain coupling (see Fig. 16 in the Appendix). Furthermore, it can be seen that there are four nodes corresponding to a phase shift of 4π in the mode $\omega_o^{(s)}(0)$ and the mode $\omega_o^{(a)}(0)$, respectively, which indicates there are four symmetric ($g_1^{(s)}$ - $g_4^{(s)}$) localized modes and four anti-symmetric ($g_1^{(a)}$ - $g_4^{(a)}$) localized modes at $q = 0$ according to Levinsons theorem [25]. Our calculation gives the eight slowly varying localized modes as shown in Figures 5 and 6, where the explicit shapes of the slow varying modes defined by $\tilde{d}_n = [d_{n-1} + 2d_n + d_{n+1}]/4$ are depicted instead of d_n themselves. For the four symmetric modes, they all have counterparts as found in polyacetylene [10,26–29]. $g_1^{(s)}$ is the Goldstone mode corresponding to the translation of the polaron, $g_2^{(s)}$ is the Amplitude mode corresponding to the amplitude vibration of the polaron, $g_3^{(s)}$ and $g_4^{(s)}$ are the third and fourth modes, respectively. Their energies are $\omega^2/\omega_Q^2 = 0, 0.025, 0.086$ and 0.124, and

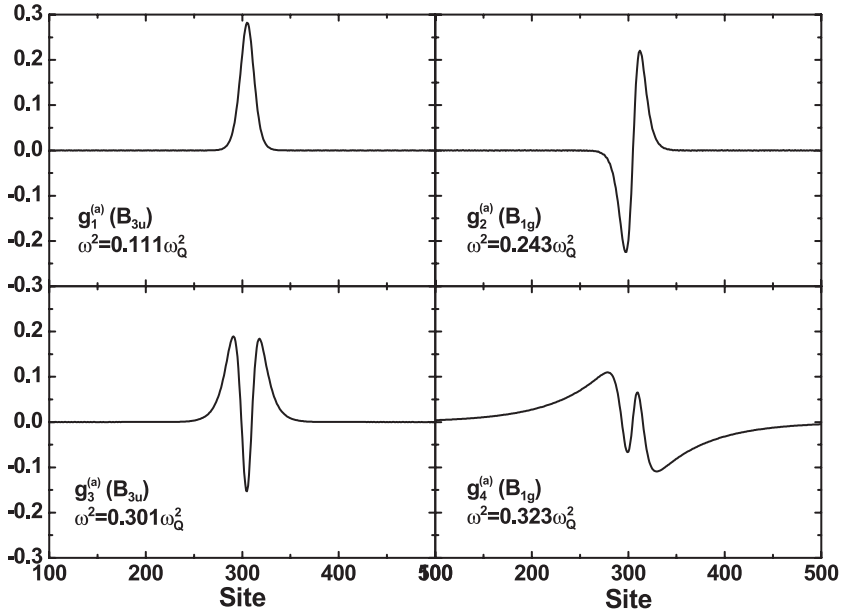

Fig. 6. Anti-symmetric localized slowly varying phonon modes ($q = 0$) around a polaron a singly-charged polyacene chain with the PBC.

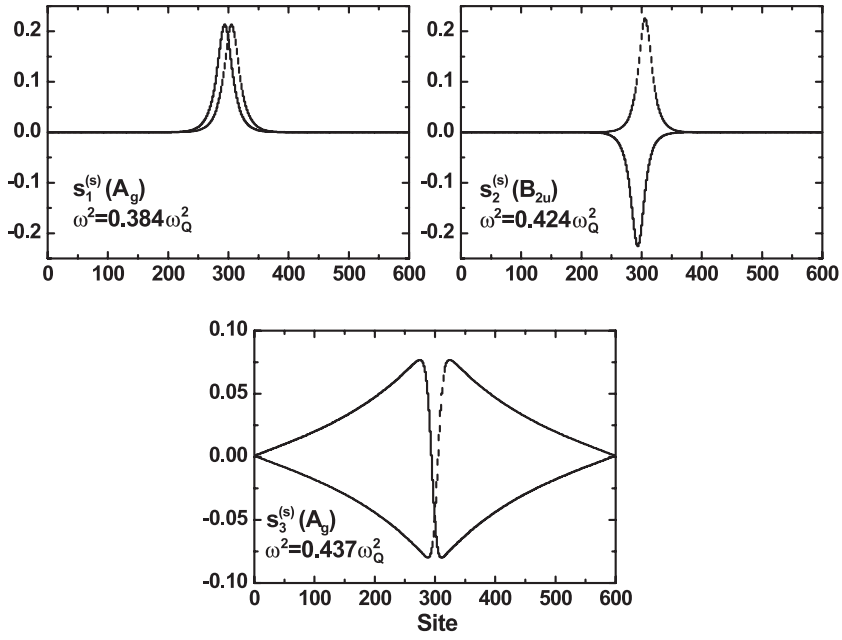

Fig. 7. Symmetric localized quickly varying phonon modes ($q = \pi/2$) around a polaron in a singly-charged polyacene chain with the PBC. The lines are defined in the text.

the corresponding irreducible representations are B_{2u}, A_g, A_g, and B_{2u}, respectively. The anti-symmetry mode $g_1^{(a)}$ of the B_{3u} symmetry is the relative amplitude vibration, and the mode $g_2^{(a)}$ of the B_{1g} symmetry is the relative position vibration between the polaron structures in the two chains of polyacene, their energies ($\omega^2/\omega_Q^2 = 0.111, 0.243$) depend sensitively on the interchain coupling $t_\perp$. The anti-symmetric modes $g_3^{(a)}$ (B_{3u}) and $g_4^{(a)}$ (B_{1g}) have the energies $\omega^2/\omega_Q^2 = 0.301$ and $\omega^2/\omega_Q^2 = 0.323$, respectively.

Except for the above eight slowly varying modes, we found five quickly varying modes: the three symmetric modes ($s_1^{(s)}$ - $s_3^{(s)}$) are shown in Figure 7 and the two anti-symmetric modes ($s_1^{(a)}$ and $s_2^{(a)}$) in Figure 8. All of these modes have a quasi-period of four sites, and can be regarded as modes at $q = \pi/2$. Therefore, for these quickly varying modes, we can define $\bar{d}_{2n+l} = (-1)^{(n)} d_{2n+l}$ to show their vibrational configurations, the solid and broken lines in Figures 7 and 8 represent $\bar{d}$ for $l = 1$ and $l = 2$, respectively. The energies and symmetries of the

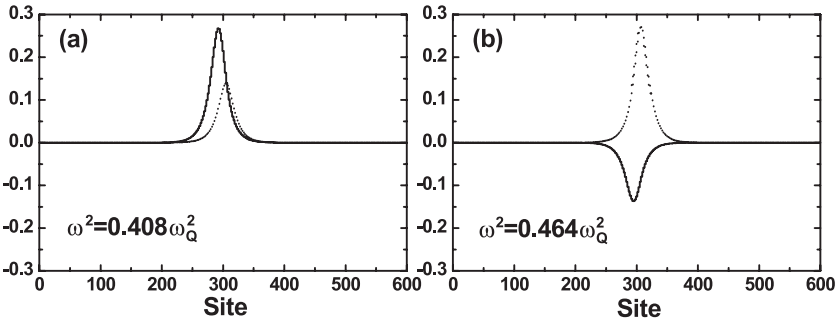

Fig. 8. Anti-symmetric localized quickly varying phonon modes ($q = \pi/2$) around a polaron in a singly-charged polyacene chain with the PBC. The lines are defined in the text.

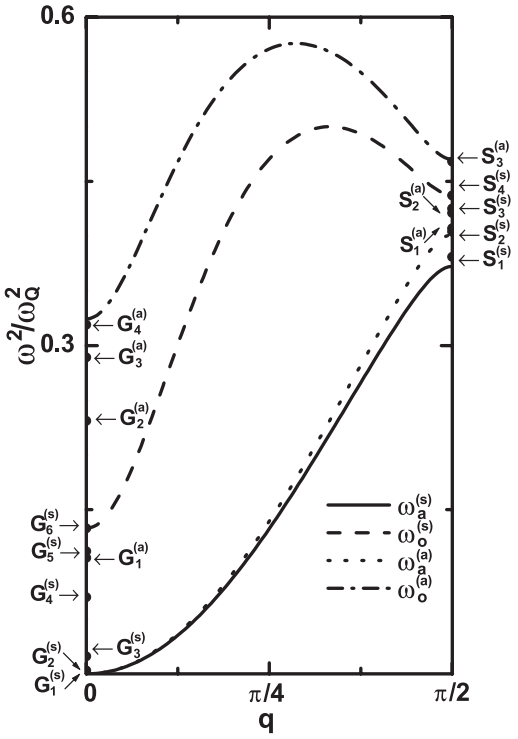

Fig. 9. The phonon spectrum of a singly-charged polyacene chain with the OBC. The energies of the localized modes around the elementary excitation are indicated by arrows.

three symmetric modes are $\omega^2/\omega_Q^2 = 0.384$ and A_g for $s_1^{(s)}$, $\omega^2/\omega_Q^2 = 0.424$ and B_{2u} for $s_2^{(s)}$, and $\omega^2/\omega_Q^2 = 0.437$ and A_g for $s_3^{(s)}$, respectively. From Figure 8, one can find that they are not symmetric in the chain direction for the two anti-symmetric modes, due to the existence of the alternate interchain coupling. The energies of these modes are $\omega^2/\omega_Q^2 = 0.408$ for $s_1^{(a)}$ and $\omega^2/\omega_Q^2 = 0.464$ for $s_2^{(a)}$, respectively.

4 Localized phonons around a charged polaron coupled with the neutral soliton

In the above section, we have discussed numerically the localized phonon modes around a polaron in a singly-charged polyacene chain with the PBC. In contrast to the case of the polyacene with the PBC, a more real polyacene chain is opened, that is, the polyacene chain with the OBC, in which each chain of the two chains in the polyacene contains odd-number unit cells, for example, nine carbon sites in each chain (totally eighteen sites) for tetracene, eleven sites in each chain (totally twenty-two) for pentacene. Therefore, it can be expected that a topological soliton distortion should occur even in a pristine polyacene chain [10,23]. Then the elementary excitations as well as the vibrational properties in a singly-charged polyacene chain with the OBC should be quite different from that of the chain with the PBC. For example, an interchain polaron coupled with the neutral soliton has been found in the singly-charged polyacene chain with the OBC (see Fig. 2) [23], in contrast with the polyacene chain with the PBC, where only an interchain coupled polaron be found (see Fig. 1). In this section, we will deal with the localized phonon modes around a charged polaron coupled with the neutral soliton in a finite poyacene chain using the same method introduced in Section 3.

In addition to three pairs of twofold-degenerate edge modes, totally, seventeen localized modes have been found around a charged polaron coupled with the neutral soliton. Figure 9 shows their energy positions in the phonon spectrum. It is clear that the bond configuration has the symmetry D_{2h}, see Figure 2. Similarly, the localized phonon modes can be identified by the four one-dimensional irreducible representations A_g, B_{1g}, B_{2u}, and B_{3u} of D_{2h} group [10], and the phonon modes corresponding to B_{2u} and B_{3u} are infrared active while the modes corresponding to A_g and B_{1g} are Raman active.

The extended modes with the lowest frequency in the optical branches in the presence of a charged polaron coupled with the neutral soliton, $\omega_o^{(s)}(0)$ and $\omega_o^{(a)}(0)$, are shown in Figure 10, the energies are $\omega^2/\omega_Q^2 = 0.134$ and 0.325 respectively, almost the same as that in the presence of a charged polaron in the polyacene chain with the PBC. It can be seen that there are six nodes corresponding to a phase shift of 6π in the mode $\omega_o^{(s)}(0)$ and four nodes corresponding to a phase shift of 4π in the mode $\omega_o^{(a)}(0)$. According to Levinsons theorem [25], there should be six symmetric ($G_1^{(s)}$ - $G_6^{(s)}$) localized modes and four anti-symmetric ($G_1^{(a)}$ - $G_4^{(a)}$) localized modes at $q = 0$. Our calculation gives both the six symmetric localized

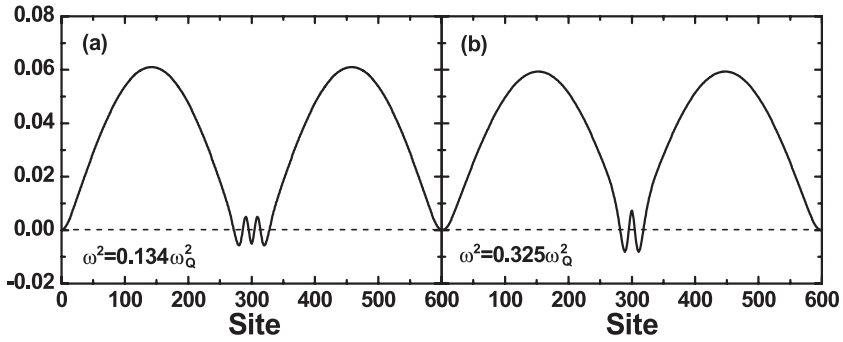

Fig. 10. The extended modes with the lowest frequency in the optical branches in the presence of a charged polaron coupled with the neutral soliton, (a) $\omega_o^{(s)}(0)$ for the symmetric optical branch and (b) $\omega_o^{(a)}(0)$ for the anti-symmetric optical branch.

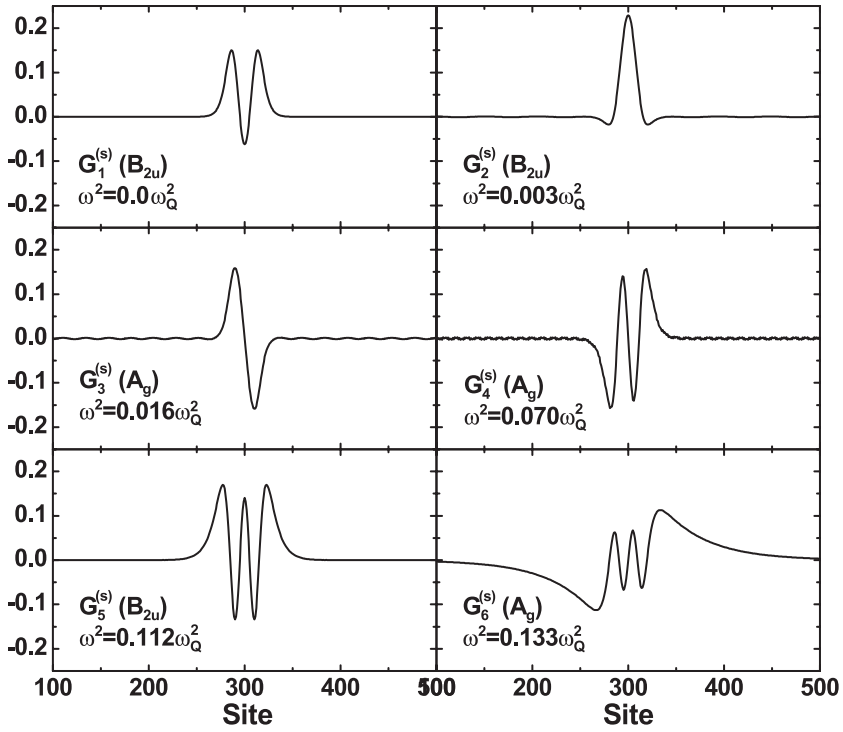

Fig. 11. Symmetric localized slowly varying phonon modes ($q = 0$) around a charged polaron coupled with the neutral soliton in a singly-charged polyacene chain with the OBC.

slowly varying modes and the four anti-symmetric localized slowly varying modes as shown in Figures 11 and 12, respectively. For the six symmetric modes, the first mode $G_1^{(s)}$, of the energy $\omega^2/\omega_Q^2 = 0.0$ and symmetry B_{2u}), is the Goldstone mode corresponding to the translation of the charged polaron together with the neutral soliton. The second mode $G_2^{(s)}$, of the energy $\omega^2/\omega_Q^2 = 0.003$ and the symmetry B_{2u}) is also a translational mode, but in which the polaron and the soliton move toward opposite directions. The frequency of this mode is quite small, which is consistent with the small binding energy between the polaron and the soliton (0.002 eV). The third one $G_3^{(s)}$, of the energy $\omega^2/\omega_Q^2 = 0.016$ and symmetry A_g), is the amplitude mode corresponding to the amplitude vibration of both the polaron and the soliton. Its frequency is smaller than that of the amplitude mode $g_2^{(s)}(\omega^2/\omega_Q^2 = 0.025)$ in the presence of an insolated polaron, and that of the amplitude mode $g_2^{(s)}(\omega^2/\omega_Q^2 = 0.097)$ in the presence of an insolated soliton [10]. The energies of the other three modes $G_{4,5,6}^{(s)}$ are $\omega^2/\omega_Q^2 = 0.070, 0.112$, and 0.133, and their symmetries are A_g, B_{2u}, and A_g, respectively. For the four anti-symmetric localized modes, shown in Figure 12, one can find that the shapes of these anti-symmetric modes around a charged polaron coupled with the neutral soliton are quite similar as those around an isolated polaron in the polyacene chain with the PBC in Figure 6. This may imply that the potential induced by the polaron is dominant, compared with that induced by the soliton. The anti-symmetric mode $G_1^{(a)}$ of the symmetry B_{1g} is the

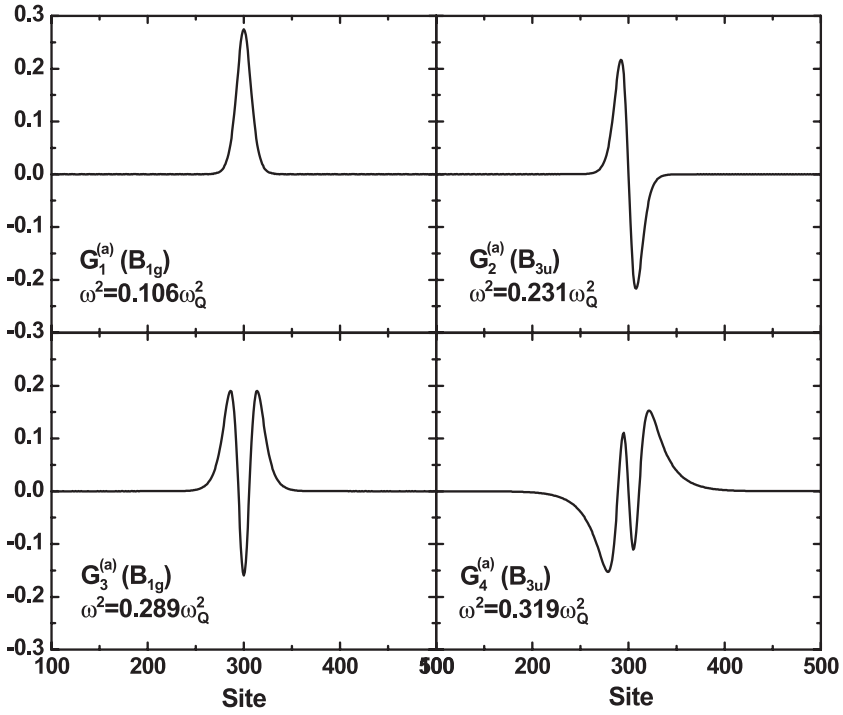

Fig. 12. Anti-symmetric localized slowly varying phonon modes ($q = 0$) around a charged polaron coupled with the neutral soliton in a singly-charged polyacene chain with the OBC.

relative position vibration of the polaron structures in the two chains of polyacene, the mode $G_2^{(a)}$ of the symmetry B_{3u} is the relative amplitude vibration of the polaron structures in the two chains, and $G_3^{(a)}$ of the symmetry B_{1g} and $G_4^{(a)}$ of the symmetry B_{3u} are the third and fourth modes, their energies $\omega^2/\omega_Q^2 = 0.106$, 0.231, 0.289, 0.319 depends sensitively on the interchain coupling $t_\perp$. It should be stressed that the energies are slightly smaller than those anti-symmetric modes around an isolated polaron, though they have similar vibrational shapes, which should result from the effect of the soliton. Also, due to the existence of the soliton, the frequency of the relative amplitude vibration mode $G_2^{(a)}$ is greater than that of the relative position vibration mode $G_1^{(a)}$, which is different from the case for an isolated polaron, i.e., the frequency of the relative amplitude vibration mode $g_1^{(a)}$ is smaller than that of the relative position vibration mode $g_2^{(a)}$. In the case for an isolated soliton, only one anti-symmetric mode $g_1^{(a)}$ is found, which corresponds to relative position vibration of the soliton. This mode is not found in the case for the coupled charged polaron and soliton. Again, it implies that the characteristic of the soliton is not distinct in this complex case. The anti-symmetric modes to be similar as $G_5^{(s)}$ and $G_6^{(s)}$ are not found, due to the strong interchain coupling, and may appear in the system with a weak interchain coupling.

In addition to the above ten slowly varying modes, we found seven quickly varying modes: four symmetric modes ($S_1^{(s)}$ - $S_4^{(s)}$) and three anti-symmetric mode ($S_1^{(a)}$ - $S_3^{(a)}$). All of these modes, shown in Figures 13 and 14, have a quasi-period of four sites, and can be regarded as modes at $q = \pi/2$. The energies and symmetries are $\omega^2/\omega_Q^2 = 0.381$ and A_u for $S_1^{(s)}$, $\omega^2/\omega_Q^2 = 0.404$ and B_{2u} for $S_2^{(s)}$, $\omega^2/\omega_Q^2 = 0.425$ and A_u for $S_3^{(s)}$, and $\omega^2/\omega_Q^2 = 0.437$ and B_{2u} for $S_4^{(s)}$, respectively. The mode $S_2^{(s)}$ is appeared at the middle of the phonon gap ($\omega^2/\omega_Q^2 = 0.370$ for $\omega_a^{(s)}(\pi/2)$ and $\omega^2/\omega_Q^2 = 0.438$ for $\omega_o^{(s)}(\pi/2)$) at $q = \pi/2$ and has the peculiar property that all even atoms are almost fixed while odd atoms oscillate in alternate directions. This mode is nothing but the staggered mode found in polyacetylene [11]. And the mode $S_4^{(s)}$, whose energy is just below $\omega_o^{(s)}(\pi/2)$, the edge of optical phonon at $q = \pi/2$. The anti-symmetric modes have energies and symmetries $\omega^2/\omega_Q^2 = 0.407$ and B_{3u} for $S_1^{(a)}$, $\omega^2/\omega_Q^2 = 0.421$ and B_{1g} for $S_2^{(a)}$, and $\omega^2/\omega_Q^2 = 0.468$ and B_{3u} for $S_3^{(a)}$, respectively. Compared with the neutral polyacene, the modes $t_1^{(a)}$ and $t_2^{(a)}$ that have a quasi-period of seven sites [10] are not found in this case, for which the reason is unknown.

Finally, we would like to point out that there exist three pairs of edge phonon modes, shown in Figure 15, since we are considering a finite-length polymer chain. All these edge modes are located above the optical phonon continuum bands and each pair contains one mode around the left end and its counterpart around the right end. A recombination of these degenerate modes gives one pair ($\omega^2/\omega_Q^2 = 0.510$) with A_g and B_{2u} symmetries and the other two pairs ($\omega^2/\omega_Q^2 = 0.578$ and 0.603) have B_{1g} and

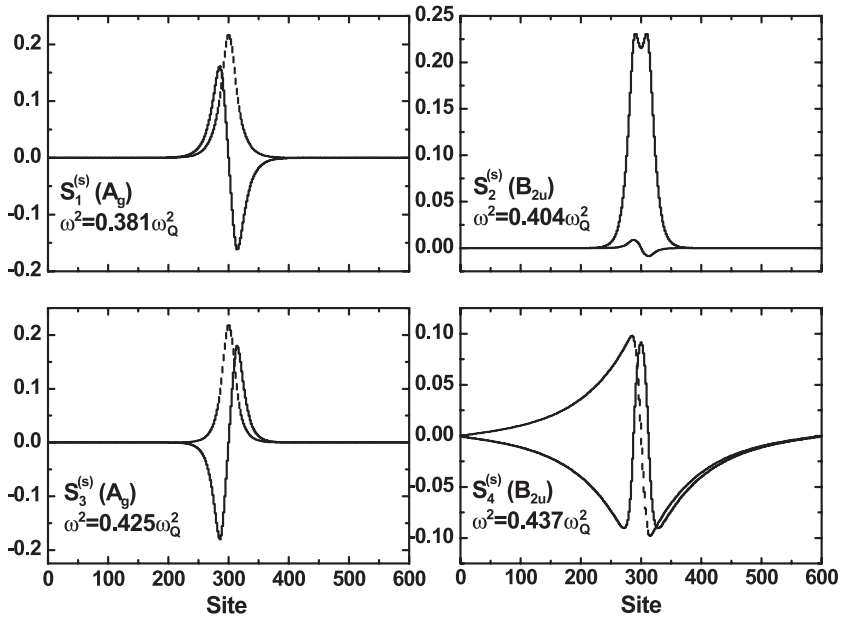

Fig. 13. Symmetric localized quickly varying phonon modes ($q = \pi/2$) around a charged polaron coupled with the neutral soliton in a singly-charged polyacene chain with the OBC.

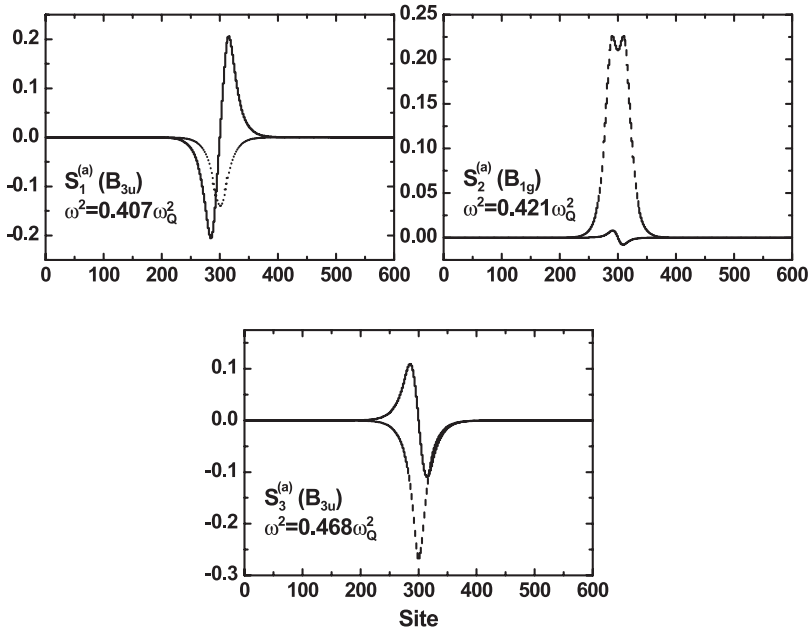

Fig. 14. Anti-symmetric localized quickly varying phonon modes ($q = \pi/2$) around a charged polaron coupled with the neutral soliton in a singly-charged polyacene chain with the OBC.

B_{2u} symmetries. In total, three edge modes are infrared active while the other three are Raman active.

5 Summary

In this paper, we have investigated the vibrational properties of polyacene. While the phonon spectrum of an uniform dimerized polyacene is given analytically, we obtain numerically all localized phonons around the elementary excitations in a singly-charged polyacene chain both with the PBC and the OBC. The result shows that the optical branches are strongly split due to the interchain interactions, but the acoustic branches are affected slightly. There have been found totally thirteen localized phonon modes around the charged polaron in the chain with the PBC. Among them, eight are slowly varying modes and five are fast varying modes. Except for two asymmetric modes which are both infrared active and Raman active, the other eleven localized modes are identified with one of the four irreducible representations of the D_{2h} group in which five (three B_{2u} and two B_{3u}) modes are infrared

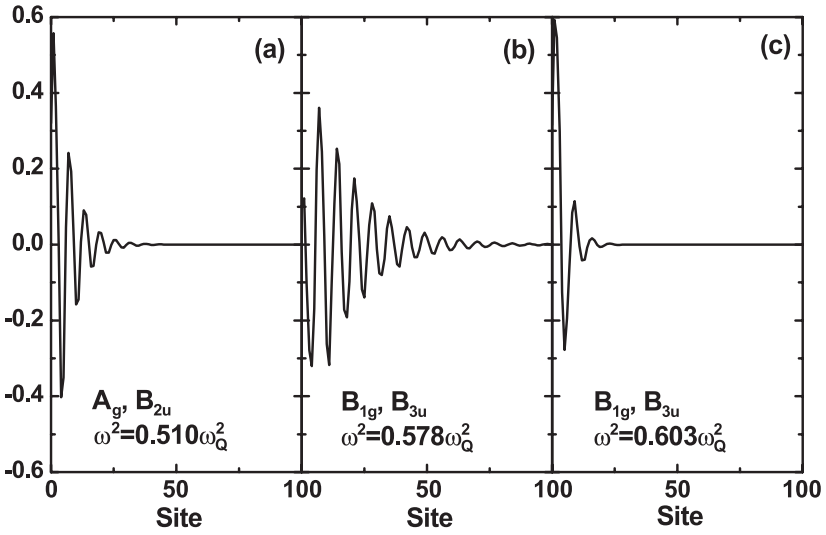

Fig. 15. Three pairs of edge phonon modes. Each pair contains one mode around the left end (shown here) and one around the right end (not shown).

active, six (four A_g and two B_{1g}) modes are Raman active. Furthermore, we investigate the localized vibrational modes around a charged polaron coupled with a neutral soliton in a singly-charged polyacene chain with the OBC, and the coupling effect between self-trapping excitations on the phonon spectra is discussed. There are seventeen localized phonon modes around the complex of polaron and soliton, among which nine modes (five B_{2u} and four B_{3u}) are infrared active, and eight modes (five A_g and three B_{1g}) are Raman active. The shapes of the localized phonons shows mainly the characteristic of polaron for the case of a charged polaron coupled with a neutral soliton, however, the number and frequencies of the localized modes are quite different from those for the case of an isolated polaron. Additionally, we find three pairs of edge phonon modes, since we are considering a finite-length polymer chain for the case of a charged polaron coupled with a neutral soliton, all are quickly varying modes, and both infrared and Raman active. As is well known, the localized phonon modes can be considered the fingerprint [11] of localized excitations in polymers, therefore, the results obtained in the present investigation will be useful to identify the characteristic of elementary excitations in polyacene.

This work was supported by National Natural Science Foundation of China (Nos. 90403110, 10204005, 10374017, and 10321003) and the State Ministry of Education of China (No. 20020246006).

Appendix: Extended phonon spectra

Due to the translational symmetry, the Peierls ground state of a neutral polyacene chain with the PBC has a dimerized lattice configuration, that is, $u_{j,n} = (-1)^n u_0^{(j)}$. Let $\Delta_j = 4\alpha u_0^{(j)}$, $\lambda = 2\alpha^2/\pi t_0 K$, and $t_1 = t_2 = t_\perp/2$, and making Fourier transformation to the electron operator, we have

$$H = \sum_{k,\sigma}{}' \Phi_{k,\sigma}^\dagger \begin{bmatrix} h_{1k} & -t_\perp(1+\sigma_1)/2 \\ -t_\perp(1+\sigma_1)/2 & h_{2k} \end{bmatrix} \Phi_{k,\sigma} + \frac{N}{4\pi t_0 \lambda}(\Delta_1^2 + \Delta_2^2), \quad \text{(A.1)}$$

where

$$\Phi_{k,\sigma} = \begin{pmatrix} \Phi_{1,k,\sigma} \\ \Phi_{2,k,\sigma} \end{pmatrix}, \quad \Phi_{j,k,\sigma} = \begin{pmatrix} c_{j,k,\sigma} \\ c_{j,k+\pi,\sigma} \end{pmatrix},$$
$$h_{j,k} = \begin{pmatrix} -2t_0 \cos k & -i\Delta_j \sin k \\ i\Delta_j \sin k & 2t_0 \cos k \end{pmatrix}, \quad \text{(A.2)}$$

and σ_1 is the Pauli matrix. The prime in equation (A.1) indicates that the summation for index k runs over the reduced Brillouin zone, i.e., $k \in (-\pi/2, \pi/2]$ for an infinite-long polyacene chain. The diagonalization of the Hamiltonian (A.1) gives the eigenenergies and eigenfunctions. Due to the electron-hole symmetry, it is clear that the eigenstates appear in pairs, with one positive and one corresponding negative energy states. In the case for an infinite polyacene ($t_1 = t_2 = t_\perp/2$), the energy spectrum is same either in the alternate *cis*-phase $\Delta_1 = \Delta_2 = \Delta_0$ or in the *trans*-phase $\Delta_1 = -\Delta_2 = \Delta_0$ configurations,

$$\varepsilon_k = \pm E_k \pm t_\perp/2, \quad \text{(A.3)}$$

here

$$E_k = \sqrt{4t_0^2 \cos^2 k + \Delta_0^2 \sin^2 k + t_\perp^2/4}\ . \quad \text{(A.4)}$$

However, for a finite polyacene chain, the bond configuration will always be in the *cis*-phase since the edge bonds should be short ones, which is similar as the case for single

polyacetylene chain [23]. Therefore, we will only consider the *cis*-phase in below. At the *cis*-phase, we consider a small departure $d_{j,n}$ of atoms from its equilibrium configuration, that is $u_{j,n} = u_0 + (-1)^n d_{j,n}$, then the perturbed electronic Hamiltonian due to the departures $\{d_{j,n}\}$ is

$$H_e^{'} = -\alpha \sum_{j,n,\sigma} (-1)^n (d_{j,n} + d_{j,n+1})(c^{\dagger}_{j,n,\sigma} c_{j,n+1,\sigma} + \text{h.c.}). \tag{A.5}$$

Making Fourier transformation

$$\begin{aligned} d_{j,n} &= \sum_q e^{-iqn} d_{j,q} \\ &\equiv \sum_q{}' \, e^{-iqn}[\eta_{j,q} + (-1)^n \xi_{j,q}], \end{aligned} \tag{A.6}$$

together with that of electronic operators, and using a reduced Brillioun zone, we have

$$H_e^{'} = -4i\alpha \sum_{j,k,q,\sigma}{}' \Phi^{\dagger}_{j,k,\sigma} D_{j,k,q} \Phi_{j,k-q,\sigma}, \tag{A.7}$$

where

$$D_{j,k,q} = \begin{bmatrix} \xi_{j,q} \sin\frac{q}{2} \cos(k - \frac{q}{2}) & \eta_{j,q} \cos\frac{q}{2} \sin(k - \frac{q}{2}) \\ -\eta_{j,q} \cos\frac{q}{2} \sin(k - \frac{q}{2}) & -\xi_{j,q} \sin\frac{q}{2} \cos(k - \frac{q}{2}) \end{bmatrix}. \tag{A.8}$$

The first order of the elastic energy is given as

$$E_p^{(1)} = \frac{K}{2\alpha} \Delta_0 \sum_{j,n} (d_{j,n} + d_{j,n+1}) = \frac{NK}{\alpha} \Delta_0 (\eta_{1,0} + \eta_{2,0}). \tag{A.9}$$

The condition for the total energy to be minimized is that the first order perturbation of $H_e^{'} + H_p$ is equal to zero, from which we can get the self-consistent equation for the dimerization Δ_0 as follows

$$\frac{1}{2\lambda} = \int_0^{\pi/2} \frac{2t_0 \sin^2 k}{E_k} dk. \tag{A.10}$$

The solution of the self-consistent equation is shown in Figure 16. The dimerization is reduced when the interchain coupling becomes large, and there will be no dimerization when the interchain coupling $t_\perp$ beyond t_0.

Having found the equilibrium condition equation (A.10), we can get the total energy of the system by calculating further the second order perturbation. The second order of the electronic energy is given by the formula

$$E_e^{(2)} = \sum_e \frac{|\langle e|H_e^{'}|G\rangle|^2}{E_g^{(0)} - E_e^{(0)}}, \tag{A.11}$$

the second order of the elastic energy is given by

$$E_p^{(2)} = 2NK \sum_{j,q}{}' \left(\cos^2\frac{q}{2} \eta^*_{j,q} \eta_{j,q} + \sin^2\frac{q}{2} \xi^*_{j,q} \xi_{j,q} \right), \tag{A.12}$$

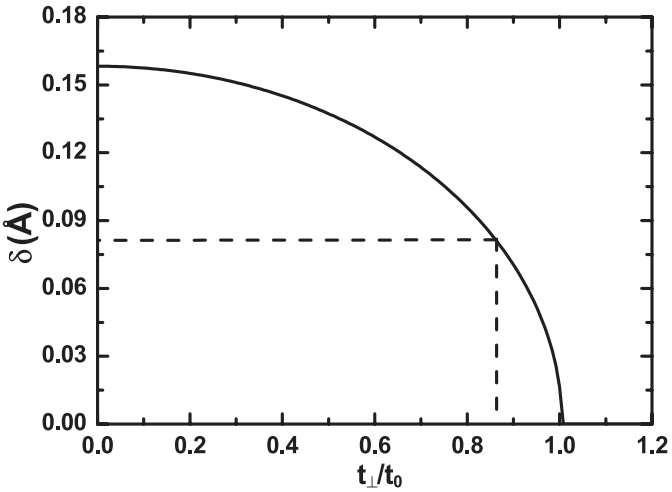

Fig. 16. The dependence of the dimerization parameter $\delta = \Delta_0/2\alpha$ on the interchain coupling $t_\perp$. The dash line corresponds to the parameters we adopted in this paper.

and the kinetic energy of the system is as follow

$$E_k^{(2)} = \frac{1}{2} NM \sum_{j,q}{}' (\dot{\eta}^*_{j,q} \dot{\eta}_{j,q} + \dot{\xi}^*_{j,q} \dot{\xi}_{j,q}). \tag{A.13}$$

It is clear that we can define symmetric and anti-symmetric vibrational variables as follows

$$\begin{aligned} \xi_q^{(s)} &= \frac{1}{\sqrt{2}} (\xi_{1,q} + \xi_{2,q}), \\ \xi_q^{(a)} &= \frac{1}{\sqrt{2}} (\xi_{1,q} - \xi_{2,q}), \\ \eta_q^{(s)} &= \frac{1}{\sqrt{2}} (\eta_{1,q} + \eta_{2,q}), \\ \eta_q^{(a)} &= \frac{1}{\sqrt{2}} (\eta_{1,q} - \eta_{2,q}), \end{aligned} \tag{A.14}$$

and the symmetric and anti-symmetric vibrations are independent, which is a result of the lattice at *cis*-phase. Now we can write the total energy till the second order of the lattice derivations.

$$\begin{aligned} E_t/N = E_0(\Delta_0) &+ \frac{1}{2} M \sum_{q,\kappa}{}' \begin{pmatrix} \dot{\xi}_q^{(\kappa)*} & \dot{\eta}_q^{(\kappa)*} \end{pmatrix} \begin{pmatrix} \dot{\xi}_q^{(\kappa)} \\ \dot{\eta}_q^{(\kappa)} \end{pmatrix} \\ &+ 2K \sum_{q,\kappa}{}' \begin{pmatrix} \xi_q^{(\kappa)*} & \eta_q^{(\kappa)*} \end{pmatrix} \begin{pmatrix} 2a_1^{(\kappa)}(q) & c^{(\kappa)}(q) \\ c^{(\kappa)*}(q) & 2a_2^{(\kappa)}(q) \end{pmatrix} \begin{pmatrix} \xi_q^{(\kappa)} \\ \eta_q^{(\kappa)} \end{pmatrix}, \end{aligned} \tag{A.15}$$

where $\kappa = s, a$. For the symmetric branches

$$a_1^{(s)}(q) = \frac{1}{2}\sin^2\frac{q}{2}\Bigg\{1 - 2\lambda t_0 \int_{-\pi/2}^{\pi/2} dk \cos^2\left(k - \frac{q}{2}\right) \frac{E_k E_{k-q} - \Lambda_{k,q} + t_\perp^2/4}{E_k E_{k-q}(E_k + E_{k-q})}\Bigg\},$$

$$a_2^{(s)}(q) = \frac{1}{2}\cos^2\frac{q}{2}\Bigg\{1 - 2\lambda t_0 \int_{-\pi/2}^{\pi/2} dk \sin^2\left(k - \frac{q}{2}\right) \frac{E_k E_{k-q} + \Lambda_{k,q} + t_\perp^2/4}{E_k E_{k-q}(E_k + E_{k-q})}\Bigg\},$$

$$c^{(s)}(q) = -i\lambda t_0^2 \Delta_0 \sin q \int_{-\pi/2}^{\pi/2} dk \frac{\sin^2(2k-q)}{E_k E_{k-q}(E_k + E_{k-q})}, \quad \text{(A.16)}$$

and for the anti-symmetric branches

$$a_1^{(a)}(q) = \frac{1}{2}\sin^2\frac{q}{2}\Bigg\{1 - 2\lambda t_0 \int_{-\pi/2}^{\pi/2} dk \cos^2\left(k - \frac{q}{2}\right) \times \frac{(E_k E_{k-q} - \Lambda_{k,q} - t_\perp^2/4)(E_k + E_{k-q})}{E_k E_{k-q}[(E_k + E_{k-q})^2 - t_\perp^2]}\Bigg\},$$

$$a_2^{(a)}(q) = \frac{1}{2}\cos^2\frac{q}{2}\Bigg\{1 - 2\lambda t_0 \int_{-\pi/2}^{\pi/2} dk \sin^2\left(k - \frac{q}{2}\right) \times \frac{(E_k E_{k-q} + \Lambda_{k,q} - t_\perp^2/4)(E_k + E_{k-q})}{E_k E_{k-q}[(E_k + E_{k-q})^2 - t_\perp^2]}\Bigg\},$$

$$c^{(a)}(q) = -\lambda t_0 \sin q \int_{-\pi/2}^{\pi/2} dk \sin(2k-q) \times \Bigg\{\frac{i t_0 \Delta_0 \sin(2k-q)(E_k + E_{k-q})}{E_k E_{k-q}[(E_k + E_{k-q})^2 - t_\perp^2]} \times \frac{(E_k - E_{k-q}) t_\perp^2/4}{E_k E_{k-q}[(E_k + E_{k-q})^2 - t_\perp^2]}\Bigg\}, \quad \text{(A.17)}$$

where $\Lambda_{k,q} = 4t_0^2 \cos k \cos(k-q) - \Delta_0^2 \sin k \sin(k-q)$. Then we have the phonon spectra as

$$[\omega^{(\kappa)}(q)]^2 = \omega_Q^2 \Bigg\{a_1^{(\kappa)}(q) + a_2^{(\kappa)}(q) \pm \sqrt{|c^{(\kappa)}(q)|^2 + \left[a_1^{(\kappa)}(q) - a_2^{(\kappa)}(q)\right]^2}\Bigg\}, \quad \text{(A.18)}$$

where $+(-)$ corresponds to the optical (acoustic) branches. The dispersion relation of the lattice vibrations for the model with those adopted parameters are shown in Figure 3 as those lines. From that figure, one can find that the two optical branches are strongly split, arising from the interchain interactions, while the two acoustic branches are slightly different at Brillouin zone boundary. Moreover, it is clear that there are no gap between the optical and acoustic branches for both symmetric and anti-symmetric spectra.

From equations (A.16−A.18), we can calculate the frequency of the phonon mode with $q = 0$ ($\omega_o^{(\kappa)}(0)$) and the phonon gap at the Brillouin zone boundary $q = \pi/2$ ($\Delta_g = \omega_o^{(\kappa)}(\pi/2) - \omega_a^{(\kappa)}(\pi/2)$). The critical point for a gap appearing between acoustic and optical branches is at $\omega_o^{(\kappa)}(\pi/2) = \omega_a^{(\kappa)}(\pi/2)$.

References

1. *Primary photoexcitations in conjugated polymers*, edited by N.S. Sariciftci (World Scienctific, Singapore, 1997)
2. A.J. Heeger, S. Kivelson, J.R. Schrieffer, W.P. Su, Rev. Mod. Phys. **60**, 781 (1988)
3. I.H. Campbell, D.L. Smith, Solid State Physics **55**, 1 (2001)
4. F. Garnier, R. Hajlaoui, A. Yassar, P. Srivastava, Science **265** 1684 (1994)
5. J.H. Burroughes et al., Nature **347**, 539 (1990)
6. J.J.M. Halls et al., Nature **376**, 500 (1995)
7. G. Yu, J. Gao, J.C. Hummelen, F. Wudl, A.J. Heeger, Science **270**, 1789 (1995)
8. N. Tessler, G.J. Denton, R.H. Friend, Nature **382**, 695 (1996)
9. J. Sinova, J. Schliemann, A.S. Núñez, A.H. MacDonald, Phys. Rev. Lett. **87**, 226802 (2001)
10. Y.J. Wu, H. Zhao, Z. An, C.Q. Wu, J. Phys.: Condens. Matter **14**, L341 (2002)
11. H. Jiang, X.H. Xu, X. Sun, K. Yonemitsu, Chin. Phys. Lett. **16**, 836 (1999)
12. L. Salem, H.C. Longuet-Higgins, Proc. R. Soc. London Ser. A **235**, 435 (1960)
13. S. Kivelson, O.L. Chapman, Phys. Rev. B **28**, 7236 (1983)
14. M.H. Whangbo, R. Hoffman, R.B. Woodward, Proc. R. Soc. London Ser. A **366**, 23 (1979)
15. K. Tanaka, K. Ozheki, S. Nankai, T. Yamabe, H. Shirakawa, Phys. Chem. Solids **44**, 1069 (1983)
16. A.L.S. da Rosa, C.P. de Melo, Phys. Rev. B **38**, 5430 (1988)
17. B. Srinivasan, S. Ramasesha, Phys. Rev. B **57**, 8927 (1998)
18. C. Raghu, Y.A. Pati, S. Ramasesha, Phys. Rev. B **65**, 155204 (2002)
19. I. Bozovic, Phys. Rev. B **32**, 8136 (1985)
20. M.K. Sabra, Phys. Rev. B **53**, 1269 (1996)
21. Z.J. Li, H.Q. Lin, K.L. Yao, Z. Phys. B **104**, 77 (1997)
22. Z.J. Li, H.B. Xu, K.L. Yao, Mod. Phys. Lett. B **11**, 477 (1997)
23. Z. An, C.Q. Wu, Int. J. Mod. Phys. B **17**, 2023 (2003)
24. H. Zhao, Z. An, C.Q. Wu, Synthetic Met. **135**, 505 (2003)
25. N. Levinson, Kgl. Danske Videnskab. Selskab, Mat.-Fys. Medd. **25**, 9 (1949)
26. C.Q. Wu, X. Sun, R. Fu, Chin. Phys. Lett. **2**, 561 (1985)
27. X. Sun, C.Q. Wu, X.C. Shen, Solid State Commun. **56**, 1039 (1985)
28. K.A. Chao, Y. Wang, J. Phys. C **18**, L1127 (1985)
29. A. Terai, Y. Ono, J. Phys. Soc. Jpn **55**, 213 (1986)
30. W.P. Su, Solid State Commun. **35**, 899 (1980)